Cherenkov Radiation from Josephson Fluxons

A. V. Ustinov[1], E. Goldobin[2], G. Hechtfischer[1], N. Thyssen[2], A. Wallraff[1], R. Kleiner[1], and P. Müller[1]

[1] Physikalisches Institut III, Universität Erlangen-Nürnberg, D-91058 Erlangen, Germany
[2] Institut für Schicht- und Ionentechnik, Forschungszentrum Jülich, D-52425 Jülich, Germany

Abstract: Josephson fluxons can generate Cherenkov radiation if they move with a velocity larger than the lowest phase velocity of Josephson plasma waves in the junction. This condition can not be realized in conventional one-dimensional long Josephson junctions. Nevertheless, Cherenkov radiation can occur from fluxons moving in more complex Josephson structures such as stacked Josephson junctions. We discuss the physics of this interesting phenomenon and present experimental data obtained with two different superconducting systems, namely artificially prepared Nb-Al-AlO_x-Nb stacks and naturally layered $Ba_2Sr_2CaCu_2O_{8+y}$ single crystals. These experiments, supported by numerical calculations using the model of inductive coupling between the junctions, well agree with theoretical predictions.

1 Introduction

Josephson fluxons, often also called Josephson vortices or Josephson solitons, appear in various contexts within nonlinear physics, superconductivity, and high-frequency device applications [1–3]. A fluxon in a long Josephson junction accounts for a circular supercurrent which yields the magnetic flux of one flux quantum $\Phi_0 = h/2e = 2.07 \times 10^{-15}$ Wb located between two superconducting electrodes of the junction. In many cases fluxon dynamics is similar to the dynamics of a relativistic particle, for which the role of the velocity of light plays the maximum velocity of electromagnetic wave propagation in the junction, also called Swihart velocity. Typically, this velocity is by about two orders of magnitude smaller than the velocity of light in vacuum.

The appearance of a fluxon in a long Josephson junction can be understood from Fig. 1. This figure sketches the cross view of the junction in the plane perpendicular to the external magnetic field H. Josephson tunnel barrier is a thin layer of insulator (I) between two superconducting electrodes (S). Due to the Meissner effect, the external field is screened by circulating supercurrents and it penetrates inside a bulk superconductor to the distance known as the London penetration depth, λ_L. Typically, λ_L is of the order of 100 nm. In the region of the Josephson barrier the screening effect is weakened, thus the magnetic field penetration distance is larger. This distance is called the Josephson penetration depth λ_J. Its value depends on the strength of the Josephson coupling (determined by the thickness of the tunnel barrier) and typically is of the order of some μm. We will be interested here

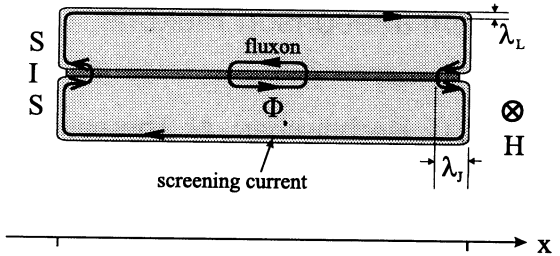

Figure 1
Schematic cross section of a long Josephson junction with a magnetic field H applied perpendicular to the plane of the picture; dimensions are not to scale.

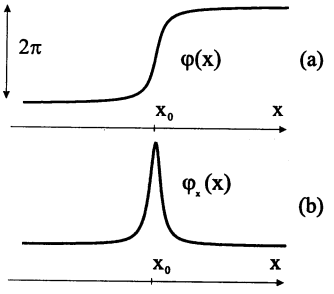

Figure 2
(a) Fluxon in a long Josephson junction accounts for a 2π kink in the phase difference $\varphi(x)$ with (b) the self-generated magnetic field proportional to $\varphi_x(x)$.

in the case when the junction is "long", so that the Josephson barrier extends over the distance L considerably larger than λ_J and the junction width W is made smaller than λ_J.

Due to the influence of the bias current flowing across the Josephson junction, the screening current tangle at the junction edge may become unstable and form a closed loop which enters the interior of the junction. This circulating supercurrent is often called Josephson vortex, and the magnetic flux generated by the vortex is equal to Φ_0.

Mathematically, the fluxon corresponds to a 2π kink of the quantum-mechanical phase difference φ between the two superconducting electrodes of the junction. The perturbed sine-Gordon equation which describes the quasi-one-dimensional dynamics of this system [4], written in the normalized form, is

$$\varphi_{xx} - \varphi_{tt} - \sin\varphi = \alpha\varphi_t - \beta\varphi_{xxt} - \gamma. \tag{1.1}$$

Here, the subscripts denote the derivatives in x and t. Time t is measured in units of ω_0^{-1}, where ω_0 is the Josephson plasma frequency, the spatial coordinate x is measured in units of λ_J, α is a dissipative term due to quasi-particle tunneling, β is a dissipative term due to surface impedance of the superconductors, and γ is a normalized bias current density. The derivation of (1.1) is based on the Maxwell and Josephson equations and can be found, e.g., in [4]. The characteristic velocity for electromagnetic waves propagating in the junction is called the Swihart velocity, $\bar{c} = \lambda_J\omega_0$.

A quasi-linear solution of (1.1) with zero right hand side exists in the limit of small amplitudes $\varphi_0 \ll 0$ where (1.1) can be linearized. This solution corresponds to the small-amplitude waves $\varphi_{pl} = \varphi_0 e^{i(kx-\omega t)}$ with the frequency ω and the wavenumber k given by the plasma-type dispersion relation $\omega^2 = 1 + k^2$. These quasi-linear waves are usually called *Josephson plasma waves*.

An important nonlinear solution to (1.1) with zero right hand side is the *soliton*

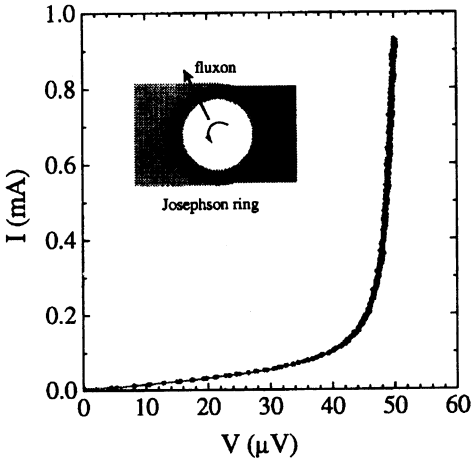

·V curve)
diameter

ar) junc-
stigation

Figure 3
Experimentally measured current-voltage characteristics (*I–V* curve) of a single fluxon in an annular Josephson junction. Junction diameter $D \approx 130\,\mu$m, temperature 5.7 K.

$$\varphi = 4\,tan^{-1}\left(exp\frac{x - x_0 - ut}{\sqrt{1-u^2}}\right) . \tag{1.2}$$

This solution describes a single fluxon as sketched in Fig. 2(a). It corresponds to a 2π-kink moving with a velocity u and located at $x = x_0$ for $t = 0$. The velocity u is measured in units of $\bar{c}$ and may assume values $0 \leq u < 1$. A unique property of the most of Josephson tunnel junctions is that the parameters α, β, and γ are small. Thus, the solution of the perturbed (1.1) can be well approximated by (1.2). To get a fluxon moving in a long Josephson junction, a dc bias current γ through the junction can be applied. The bias current acts with a Lorentz force F_γ on the fluxon and provides the energy input which is sufficient to compensate the friction force F_α) which corresponds to the α and β terms in (1.1). In the following, in the order to simplify our discussion, we will neglect the latter assuming $\beta = 0$.

According to the perturbation theory of McLaughlin and Scott [4], the soliton velocity u is determined by a balance between the losses, governed by α term, and the energy input due to the bias γ:

$$u = \frac{1}{\sqrt{1 + \left(\frac{4\alpha}{\pi\gamma}\right)^2}} \tag{1.3}$$

For low values of the bias current $u \propto \gamma/\alpha$, while for large values of γ/α the normalized velocity u asymptotically approaches unity, i.e., a fluxon behaves like *a relativistic particle* with respect to the limiting velocity $\bar{c}$. As $u \to 1$, the magnitude of the local magnetic field φ_x in the center of the fluxon increases and the fluxon width decreases, according to the well-known relativistic effect of the Lorentz contraction.

After the fluxon has passed a given point x_0 inside the junction, the phase difference $\varphi(x_0)$ shifts by 2π. A periodic fluxon motion will be accompanied by a dc voltage $V = \Phi_0/\langle\Delta T\rangle$, where $\langle\Delta T\rangle$ is the average time interval between the passing fluxons.

As an example, let us consider a special case of a ring-shaped (annular) junction geometry. An annular junction serves as an excellent model for investigation of soliton dynamics, which can be studied here under periodic boundary conditions. Due to the magnetic

flux quantization in a superconducting ring, the number of fluxons initially trapped in the annular junction is conserved. An example of experimentally measured current-voltage characteristics (I–V curve) of a single fluxon trapped in an annular Josephson junction is given in Fig. 3. A circular motion of the fluxon under the influence of a current passing through the junction induces a dc voltage proportional to its average velocity. When increasing the bias current, the fluxon velocity increases and approaches the Swihart velocity which corresponds to the dc voltage $V_1 = \Phi_0 \bar{c}/(\pi D) \approx 50\,\mu$V, with D being the junction diameter. In Fig. 3 one can see that the critical current of the annular junction with the trapped fluxon is very small, it means that we need to apply a very small force (critical current) to start the fluxon motion in this almost pinning-free system.

In conventional long junctions with open boundaries a sufficiently large external magnetic field H leads to the so-called flux-flow regime. In this mode fluxons are created at one boundary of the junction, move through the junction under the influence of the bias current, and annihilate at the other boundary. The spacing between the moving fluxons is inversely proportional to H. At large bias current, the fluxon motion with the velocity close to the Swihart velocity $\bar{c}$ is manifested experimentally by the *flux-flow step* (FFS) in the I–V characteristics [5]. For a single-barrier junction, FFS appears at the dc voltage $V_{FF} = (2\lambda_L + t)\bar{c}H$. The flux-flow regime is discussed below in relation to the measurements of $Ba_2Sr_2CaCu_2O_{8+y}$ (BSCCO) crystals.

2 Stacked Junctions

Fluxons in stacked Josephson junctions have recently become a subject of intensive theoretical and experimental investigations. The discovery of the intrinsic Josephson effect in some HTS such as BSCCO convincingly showed that these materials are essentially natural superlattices of Josephson junctions formed on the atomic scale [6–10]. The spatial period of such a superlattice is only 1.5 nm, so the Josephson junctions are packed extremely dense. The superconducting electrodes are formed by the copper oxide bilayers as thin as 0.3 nm and are separated by the non-superconducting BiO layers.

Modern thin film technology allows to grow high-quality superconducting multilayers with many Josephson tunnel barriers. Artificially prepared low-T_c stacked junctions can serve as model systems for layered high-T_c superconductors. The best multi-junction low-T_c stacks are made using Nb-Al-AlO_x-Nb junctions [11,12].

Superlattices with many Josephson layers can naturally be expected to show very complex dynamics. Therefore, it is important at first to understand in detail the dynamics of stacked junctions with very few layers.

2.1 Two Coupled Junctions

For the first time fluxon dynamics in two inductively coupled long Josephson junctions was considered theoretically by Mineev et al. [14]. The perturbation approach for small coupling has been further explored by Kivshar and Malomed [13] and Grønbech-Jensen et al. [15]. A very important step towards quantitative comparison with real experiments was made by Sakai et al. [16] who derived a model for arbitrary strong coupling between the junctions. According to that model, two stacked junctions are described by a system of coupled perturbed sine-Gordon equations

$$\begin{aligned} \frac{1}{1-S^2}\varphi^{\mathrm{A}}_{xx} - \varphi^{\mathrm{A}}_{tt} \quad &- \sin\varphi^{\mathrm{A}} - \frac{S}{1-S^2}\varphi^{\mathrm{B}}_{xx} = \alpha\varphi^{\mathrm{A}}_{tt} + \gamma^{\mathrm{A}}; \\ \frac{1}{1-S^2}\varphi^{\mathrm{B}}_{xx} - \varphi^{\mathrm{B}}_{tt} \quad &- \sin\varphi^{\mathrm{B}} - \frac{S}{1-S^2}\varphi^{\mathrm{A}}_{xx} = \alpha\varphi^{\mathrm{B}}_{tt} + \gamma^{\mathrm{B}}. \end{aligned} \tag{2.4}$$

Here $\varphi^{\mathrm{A}}(x,t)$ and $\varphi^{\mathrm{B}}(x,t)$ are the superconducting phase differences across the stacked junctions A and B, respectively, and γ^{A} and γ^{B} are the bias currents. The coupling coefficient $S = -\left[\left(\frac{t}{\lambda_{\mathrm{L}}} + \coth\frac{d}{\lambda_{\mathrm{L}}} + \coth\frac{d_{\mathrm{e}}}{\lambda_{\mathrm{L}}}\right)\sinh\frac{d}{\lambda_{\mathrm{L}}}\right]^{-1} < 0$ can be calculated from experimental parameters such as the tunnel barrier thickness t, the middle electrode thickness d, the thickness of the top and bottom electrodes d_{e}. Obviously, the coupling parameter S vanishes for $d \gg \lambda_{\mathrm{L}}$. It is associated with screening currents in superconducting electrodes which are shared by fluxons belonging to different layers. A typical experimental value for S lies in the interval from -0.2 to -0.9.

Equations (2.4) lead to two different modes, one with in-phase and another with out-of-phase oscillations in the two junctions. Recently both in-phase and out-of-phase modes were observed experimentally [17]. The similar modes have been predicted many years ago by Ngai [18] for the Josephson junction coupled with superconducting transmission line. The corresponding wave propagation velocities are $\bar{c}_- = \bar{c}/\sqrt{1-S}$ (out-of-phase) and $\bar{c}_+ = \bar{c}/\sqrt{1+S}$ (in-phase) [19].

When applying a magnetic field H parallel to the Josephson barrier, one finds the Fiske-steps in the I–V curve of stacks. Fiske-steps are caused by the resonances of linear waves on the length of the junction. In two coupled junctions one may observe two families of Fiske-steps corresponding to different modes of plasma waves. By measuring the voltage spacings between neighboring Fiske-steps $\Delta V_- = \bar{c}_-\Phi_0/(2L)$ and $\Delta V_+ = \bar{c}_+\Phi_0/(2L)$ the characteristic velocities $\bar{c}_-$ and $\bar{c}_+$ can be measured experimentally for double-junction stacks with different thickness d of the common superconducting layer [19]. With decreasing d, the coupling is increasing, thereby increasing the difference between $\bar{c}_-$ and $\bar{c}_+$. A detailed analysis of experimental data is found to be in good quantitative agreement with theory [19].

Fluxon configurations in two-stacked junction can be noted $[N|M]$ meaning N fluxons located in one LJJ and M fluxons in the other LJJ (N,$M < 0$ describe anti-fluxons). Using numerical simulations [16], it has been demonstrated that two solitary fluxons form the stable bound state $[1|1]$ with identical phases in two junctions $\varphi^{\mathrm{A}}(x,t) = \varphi^{\mathrm{B}}(x,t)$. This state has been analytically shown to be stable in the velocity range $\bar{c}_- < v < \bar{c}_+$ [20]. The coherent fluxon-antifluxon state ($[1|-1]$) which is stable up to the limiting velocity $\bar{c}_-$ has been reported in experiments by Carapella et al. [21]. The asymmetric $[1|0]$ fluxon mode in two-fold stack leads to Cherenkov radiation which will be discussed in Section 3.

2.2 Multi-Layer Stacked Junctions

Josephson superlattices consisting of many stacked tunnel junctions were discussed in the literature long before they first became available for experiments [22–24]. A multi-junction stack consists of alternating superconducting and isolating layers. In a magnetic field H applied parallel to the layers, fluxons penetrate into different Josephson junctions and, under the influence of the bias current may move coherently due to the interaction of their screening currents flowing in the inner superconducting layers.

The equations for such a stacked junction system may be obtained as a generalization of the single junction sine-Gordon equation. Josephson junction stacks consisting of N junctions ($i = 1,\ldots,N$) contain $N+1$ superconducting layers. The system of coupled sine-Gordon equations which describe the Josephson phase dynamics in the stack can be written in the following form [16]

$$\frac{\Phi_0 C_i}{2\pi}\frac{\partial^2\phi_i}{\partial t^2} + \frac{\Phi_0 G_i}{2\pi}\frac{\partial\phi_i}{\partial t} = I_B - j_{c,i}\sin\phi_i + \frac{\Phi_0}{2\pi\mu_0}\sum_{j=1}^{N} F_{i,j}\frac{\partial^2\phi_j}{\partial x^2} \tag{2.5}$$

where $i = 1,2,\ldots,N$ is the junction index, ϕ_i is the superconducting phase difference on the junction number i, Φ_0 is the magnetic flux quantum. C_i, G_i, $j_{c,i}$ and I_B are the junction capacitance, quasiparticle conductance, critical current and bias current densities, respectively. The coupling between junctions i and j is defined by matrix element $F_{i,j}$ [16]. The major parameter which determines the strength of coupling between the junctions i and $i-1$ is

$$S \equiv \frac{s_i}{d'_{i,i-1}} = -\frac{\lambda_L}{\sinh\frac{d_i}{\lambda_L}\left(t + \lambda_L\coth\frac{d_{i-1}}{\lambda_L} + \lambda_L\coth\frac{d_i}{\lambda_L}\right)}\,, \tag{2.6}$$

where d_i is the thickness of the superconducting layer i between the junctions. t is the thickness of the tunnel barrier, the London penetration depth λ_L we assume both to be the same in all the layers. The strongest coupling ($|S| \to 0.5$) is achieved for $d_i \ll \lambda_L$.

Resonant modes for superlattices have been first calculated by Kleiner [25]. Similar to Fiske modes of conventional single-barrier junctions, Kleiner obtained general expressions for eigenfrequencies corresponding to standing wave patterns in the directions normal to the layers and along the layers. For $N-$junction stacks there exist N different modes [25,19]. Kleiner modes are characterized by phase shifts between Josephson oscillations in different layers. In fact, the above mentioned $\bar{c}_-$ and $\bar{c}_+$ Fiske modes of two-fold stacks are nothing else but the lowest and the highest Kleiner modes: For a two-junction stack there are only two modes possible, the symmetric mode and the antisymmetric mode.

3 Cherenkov Radiation in Stacked Junctions

In a one-dimensional Josephson junction, the phase velocity of Josephson plasma waves $u_{ph} = \omega/k$ can never be smaller than 1 (Swihart velocity in normalized units), while the fluxon velocity u can only be smaller than 1. Thus, the Cherenkov radiation condition $u_{ph} = u$ for a fluxon moving as a relativistic particle, cannot be satisfied in usual long Josephson junctions.

The idea of possible Cherenkov radiation by a fluxon moving in some more complex cases has been discussed in several theoretical papers [13,26,27]. Very recently, we reported first experimental evidences for the Cherenkov radiation [28,31]. These experiments, performed on two very different Josephson systems are discussed below. The mechanism of the phenomenon is very general: Cherenkov radiation can be generated if the fluxon velocity u becomes equal to the phase velocity $u_{ph} = \omega/k$ of linear electromagnetic waves in the system. In contrast to single-barrier long Josephson junctions, this condition can be satisfied in stacked structures.

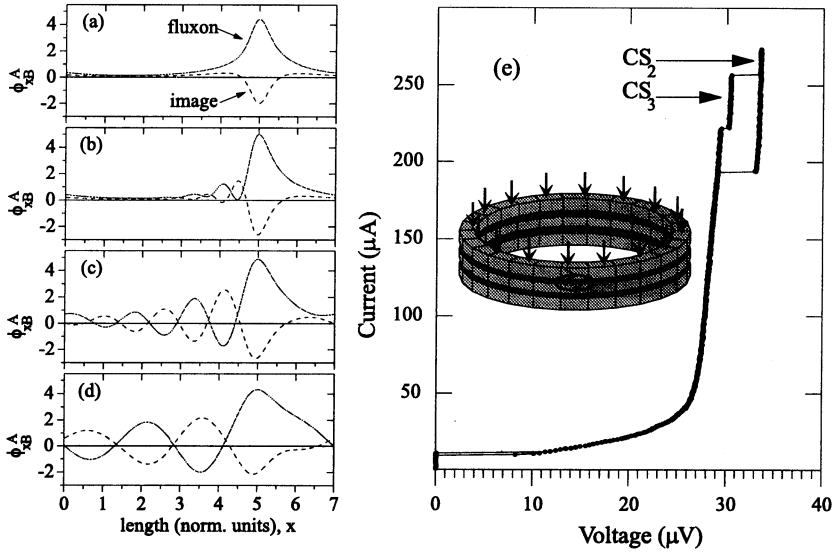

Figure 4 Simulated profiles of $\varphi_x^{A,B}(x)$ in [1|0] state of two stacked annular junctions [28]: (a) fluxon at velocity $u < c_-$, and (b), (c), and (d) with steadily increasing of u above c_-. (e) Experimental I–V characteristic of such stack in [1|0] state [28]. Cherenkov resonances are marked $CS_{2,3}$. The inset shows schematically the sample geometry.

3.1 Two Junctions: Nb-Al-AlO_x-Nb Stacks

Very clean evidence for Cherenkov radiation by a moving soliton has been found in a system of two stacked annular Josephson junctions [28]. Numerical simulations of the so called [1|0] configuration (1 soliton moving in junctions A and no soliton in junction B) shown in Fig. 4a–d demonstrate that the soliton in junction A moves together with is its image in junction B. As soon as the soliton velocity u exceeds $\bar{c}_-$, an oscillating wake corresponding to Cherenkov radiation arises behind the moving soliton and its image, as shown in Fig. 4b-d. The emitted radiation belongs to the out-of-phase mode as can be seen from Fig. 4b-d. With increasing the soliton velocity, the wavelength of the radiation increases while the amplitude and length of the wake quickly grow.

As the velocity of soliton increases, the Cherenkov radiation wake grows. If its length becomes comparable with the junction length, the radiation can form a running wave in which an integer number of Cherenkov radiation wavelengths fit into the circumference of the junction. The interaction of the running Cherenkov wave with the fluxon leads to the resonances on I–V characteristic of the system. The experimentally measured single-soliton step with Cherenkov resonances is shown in Fig. 4e. Resonances CS_2 and CS_3 are observed at $u > \bar{c}_-$ where $\bar{c}_-$ corresponds to the junction voltage of about 29μV. Numerical simulations of the I–V curve using experimental parameters demonstrated excellent agreement with measurements [28].

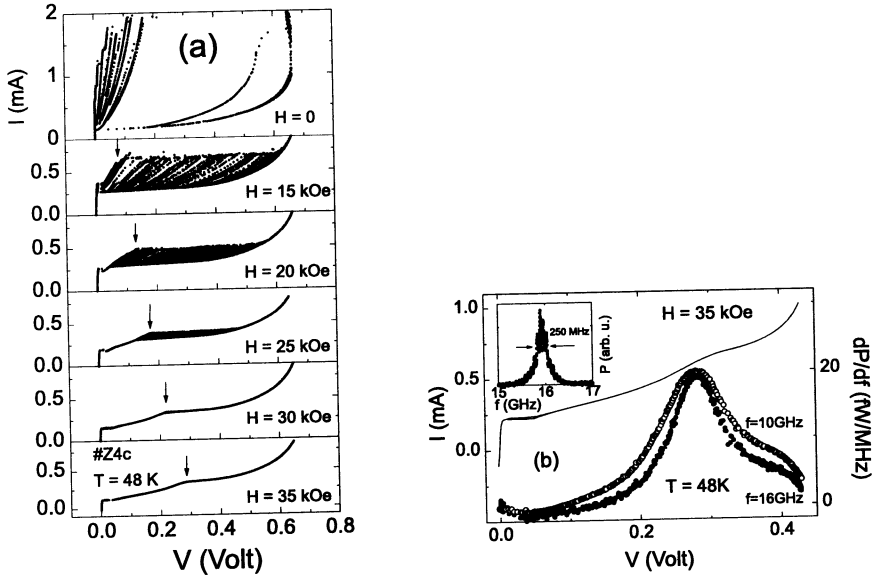

Figure 5 (a) *I–V* characteristics of a naturally grown BSCCO stack at various magnetic fields [31]. The arrow denotes the top of the flux-flow branch, i. e. the point of maximum fluxon velocity. (b) *I–V* characteristic and *non-Josephson* microwave emission vs. *V*. The form of the emission peak is almost the same for different frequencies, suggesting that the non-Josephson signal is extremely broadband [31]. The inset shows a typical spectrum of the conventional *Josephson* emission taken at 3 mV bias.

3.2 Many Junctions: $Ba_2Sr_2CaCu_2O_{8+y}$ Natural Stacks

Single crystals of BSCCO and some other materials [29] show properties expected for multi-layer stacks of Josephson junctions. Among these properties are the multi-hysteretic switching of individual tunnel junctions to gap voltages [7,8], the magnetic field dependence of the $c-$axis critical current [9] and flux-flow voltage [10,30], and Josephson radiation emission detected in several frequency bands [30]. Since it is rather difficult to measure the voltage on a single Josephson junction of atomic scale, natural stacks are usually measured in series.

An example of BSCCO stack *I–V* characteristics for magnetic fields between 20 kOe and 35 kOe is shown in Fig. 5a [31]. In zero magnetic field, the *I–V* characteristic of an intrinsic junction stack with N junctions consists of N branches which differ by the number of junctions switched to the gap state. The magnetic field primarily increases the slope of the flux-flow branch where no junction is switched to the gap [10,30]. The arrows in Fig. 5a show the characteristic flux-flow voltage which reaches 0.3 V at 35 kOe. As the stack consists of about 95 Josephson junctions this voltage corresponds to a Josephson frequency of 1.8 THz.

We observed [31] a very unusual broadband non-Josephson radiation emission from BSCCO samples shown in Fig. 5b. At the higher magnetic fields, an additional microwave

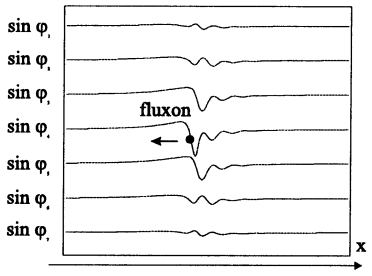

Figure 6
Spatial distribution of the supercurrents in a strongly coupled stack of seven Josephson junctions with periodic boundary conditions. A single fluxon indicated by a circle is moving in the middle junction at a velocity of 0.816 $\bar{c}$ which is higher than the lowest two mode velocities, 0.721 and 0.765 $\bar{c}$. Cherenkov radiation in the form of a trailing wave and waves induced in the neighboring junctions can clearly be seen.

emission is found at voltages much higher than the voltage of the Josephson signal illustrated in the inset of Fig. 5b. The intensity of this signal is increasing towards the top of the flux-flow branch and is by almost one order of magnitude higher than that of the Josephson signal.

Based on the magnetic field dependence of the radiation power and numerical simulations, we argue [31] that the emission is due to the Cherenkov radiation by Josephson fluxons moving in the multilayered stack. For a stack with N junctions, there are N different linear mode velocities. For strong coupling, the lowest mode velocity is about $\bar{c}/\sqrt{2}$ [30]. As soon as the fluxon velocity u rise above $\bar{c}/\sqrt{2}$ Cherenkov emission should appear. A numerical illustration of this effect in a system of 7 stacked Josephson junctions is shown in Fig. 6 [31]. Simulations are based on the coupled sine-Gordon model as described above and in [25,30]. To eliminate the influence of the boundaries, periodic boundary conditions were used. Figure 6 shows a single fluxon steadily moving in the middle junction with a velocity of 0.816 $\bar{c}$, which is above the lowest two linear mode velocities. The waves trailing the fluxon are caused by Cherenkov radiation: these waves are only observed when the lowest mode velocity of 0.721 $\bar{c}$ is exceeded! Cherenkov emission in intrinsic multi-junction stacks with large number of layers can be expected to occur simultaneously at different but close frequencies.

The non-Josephson signal was detected at frequencies that are by two orders of magnitude lower than the Josephson frequency. The occurrence of a low frequency signal can be understood as a downconverted mixing product of all the plasma waves exited by Cherenkov mechanism. The mixing of the different modes is expected in a complex and highly nonlinear system as the stacked Josephson junctions. To demonstrate this process, a stack of 21 Josephson junctions with the damping parameter $\alpha = 0.14$ and open boundary conditions was calculated numerically for the same coupling parameter as in Fig. 6. The magnetic field was chosen to give a distance between fluxons of $1.15\lambda_J$, similar to the experimental conditions. The voltage over the whole stack, taken at the boundary, was calculated for discrete time steps and was Fourier transformed to evaluate the microwave emission spectrum. Five of these spectra for different bias currents are shown in Fig. 7. For the lower two normalized bias currents, fluxons are moving slower than the lowest mode velocity. The spectrum contains mainly the Josephson signal and its second harmonic. The additional small signal at a normalized frequency of 0.1 is the fundamental cavity mode. For bias currents higher than $i = 0.560$, the fluxons in some junctions exceed the lowest mode velocity. As can be seen from Fig. 7, the Josephson signal and its harmonic are broadened, and an additional emission signal at very low frequencies appears. These simulation results, indeed, suggest that the observed non-Josephson radiation is due to the downcoversion of the multi-frequency Cherenkov emission.

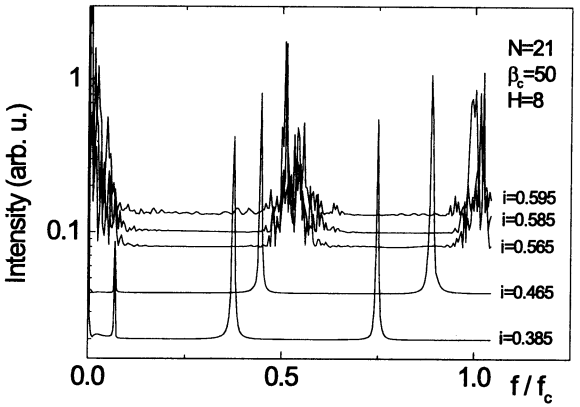

Figure 7 Fourier transforms of the voltage over a stack of 21 Jospehson junctions for five different values of normalized bias current and a normalized field of $H = 8\Phi_0/[\mu_0 B \times 1.5\text{nm}]$. For the two lower values, fluxons are slower than the lowest mode velocity. For current higher than about 0.560, fluxons move faster than the lowest mode velocity. .

4 Conclusion

We presented observations of Cherenkov radiation by Josephson fluxons moving in multilayer tunnel junctions. Experiments have been made with two different superconducting systems, namely artificially prepared Nb-Al-AlO_x-Nb stacks and naturally layered $Ba_2Sr_2CaCu_2O_{8+y}$ crystals. In the first case, Cherenkov radiation in two stacked annular Josephson junctions leads to resonances which result from interaction of Cherenkov radiation wake with a Josephson fluxon turning around the junction. Experimental data are in good quantitative agreement with the proposed model and numerical simulations. In the second case, large number of wave propagation modes, equal to the number of intrinsically stacked junctions, leads to a broad band non-Josephson emission which has been detected experimentally. These results suggest that rather unusual fluxon dynamics may take place in intrinsic junctions of high temperature superconductors.

Finally, we would like to note that Cherenkov radiation from moving fluxons may appear in various complex Josephson structures, including planar Josephson junction arrays, two-dimensional junctions and other complex systems.

Bibliography

[1] N. F. Pedersen, in: *Solitons*, S. E. Trullinger, V. E. Zakharov, V. L. Pokrovsky, eds. (Elsevier, Amsterdam, 1986), p. 469.

[2] R. D. Parmentier, in: *The New Superconducting Electronics*, H. Weinstock, R. W. Ralston, eds. (Kluwer, Dordrecht, 1993), p. 221.

[3] A. V. Ustinov, *Solitons in Josephson junctions*, to appear in Physica D (1998).

[4] D. W. McLaughlin and A. C. Scott, Phys. Rev. A **18**, 1652 (1978).

[5] T. Nagatsuma, K. Enpuku, F. Irie, and K. Yoshida, J. Appl. Phys. **54**, 3302 (1983); **56**, 3284 (1984); **58**, 441 (1985); **63**, 1130 (1988).

[6] R. Kleiner, F. Steinmeyer, G. Kunkel and P. Müller, Phys. Rev. Lett. **68**, 2394 (1992).

[7] R. Kleiner and P. Müller, Phys. Rev. B **49**, 1327 (1994).

[8] A. Yurgens, D. Winkler, N. Zavaritsky, and T. Claeson, Phys. Rev. B **53**, R8887 (1996).

[9] Yu. I. Latyshev, J. E. Nevelskaya, and P. Monceau, Phys. Rev. Lett. **77**, 932 (1996).

[10] J. U. Lee, J. E. Nordman, and G. Hohenwarter, Appl. Phys. Lett. **67**, 1471 (1995).

[11] R. Monaco and A. Oliva, Appl. Phys. Lett. **64**, 3042 (1994).

[12] H. Kohlstedt, F. König, P. Henne, N. Thyssen, and P. Caputo, J. Appl. Phys. **80**, 5512 (1996)

[13] Yu. S. Kivshar and B. A. Malomed, Phys. Rev. B **37**, 9325 (1988).

[14] M. B. Mineev, G. S. Mkrtchjan, and V. V. Schmidt, J. Low Temp. Phys. **45**, 497 (1981).

[15] N. Grønbech-Jensen, M. R. Samuelsen, P. S. Lomdahl, and J. A. Blackburn, Phys. Rev. B **42** 3976 (1990); N. Grønbech-Jensen, O. H. Olsen, and M. R. Samuelsen, Phys. Lett. A **179A**, 27 (1993).

[16] S. Sakai, P. Bodin, and N. F. Pedersen, J. Appl. Phys. **73** (1993) 2411.

[17] A. V. Ustinov, H. Kohlstedt, M. Cirillo, N. F. Pedersen, G. Hallmanns, and C. Heiden, Phys. Rev. B **48** (1993) 10614.

[18] K. L. Ngai, Phys. Rev. **182** 555 (1969).

[19] S. Sakai, A. V. Ustinov, H. Kohlstedt, A. Petraglia, and N. F. Pedersen, Phys. Rev. B **50**, 12905 (1994).

[20] N. Grønbech-Jensen, D. Cai, and M. R. Samuelsen, Phys. Rev. B **48**, 16160 (1993).

[21] G. Carapella, G. Costabile, A. Petraglia, N. F. Pedersen, and J. Mygind, Appl. Phys. Lett. **69**, 1300 (1996).

[22] P. R. Auvil and J. B. Ketterson, J. Appl. Phys. **61**, 1957 (1987).

[23] A. F. Volkov, Pis'ma Zh. Exsp. Teor. Fiz. **45**, 299 (1987) [JETP Lett. **45**, 376 (1987)]; A. F. Volkov, Pis'ma Zh. Exsp. Teor. Fiz. **50**, 127 (1989) [JETP Lett. **50**, 139 (1989)].

[24] B. A. Malomed, I. B. Khalfin, and B. Ya. Shapiro, *Sol. St. Commun.* **87**, 223 (1993).

[25] R. Kleiner, Phys. Rev. B **50**, 6919 (1994).

[26] R. G. Mints and I. B. Snapiro, Phys. Rev. B **52**, 9691 (1995).

[27] V. V. Kurin and A. V. Yulin, Phys. Rev. B **55**, 11659 (1997).

[28] E. Goldobin, A. Wallraff, N. Thyssen, and A. V. Ustinov, Phys. Rev. B **57**, 130 (1998).

[29] P. Müller, in: *Festkörperprobleme / Advances in Solid State Physics*, vol. 34, ed. by Helbig (Vieweg, Braunschweig), p.1 (1995).

[30] G. Hechtfischer, R. Kleiner, K. Schlenga, W. Walkenhorst, P. Müller, and H. L. Johnson, Phys. Rev. B **55**, 14638 (1997).

[31] G. Hechtfischer, R. Kleiner, A. V. Ustinov, and P. Mueller, Phys. Rev. Lett. **79**, 1365 (1997).